Huntingtin forms toxic NH$_2$-terminal fragment complexes that are promoted by the age-dependent decrease in proteasome activity

Hui Zhou, Fengli Cao, Zhishan Wang, Zhao-Xue Yu, Huu-Phuc Nguyen, Joy Evans, Shi-Hua Li, and Xiao-Jiang Li

Department of Human Genetics, Emory University School of Medicine, Atlanta, GA 30322

Although NH$_2$-terminal mutant huntingtin (htt) fragments cause neurological disorders in Huntington's disease (HD), it is unclear how toxic htt fragments are generated and contribute to the disease process. Here, we report that complex NH$_2$-terminal mutant htt fragments smaller than the first 508 amino acids were generated in htt-transfected cells and HD knockin mouse brains. These fragments constituted neuronal nuclear inclusions and appeared before neurological symptoms. The accumulation and aggregation of these htt fragments were associated with an age-dependent decrease in proteasome activity and were promoted by inhibition of proteasome activity. These results suggest that decreased proteasome activity contributes to late onset htt toxicity and that restoring the ability to remove NH$_2$-terminal fragments will provide a more effective therapy for HD than inhibiting their production.

Introduction

Huntington's disease (HD) is characterized by progressive and late onset neurodegeneration, which is caused by a polyglutamine (polyQ) expansion in the NH$_2$-terminal region of huntingtin (htt), a 350-kD protein of unknown function. A number of studies have shown that NH$_2$-terminal fragments of mutant htt are cytotoxic. For example, transfection of NH$_2$-terminal mutant htt causes cells to die (Cooper et al., 1998; Hackam et al., 1998; Li et al., 1999). HD transgenic mice expressing small NH$_2$-terminal htt (<171 aa) with an expanded polyQ tract show progressive neurological phenotypes and early death (Davies et al., 1997; Schilling et al., 1999).

The toxicity of NH$_2$-terminal mutant htt is also indicated by its abnormal protein conformation including misfolding, aggregation, and the formation of inclusions. Like other types of protein inclusions, polyQ-containing inclusions are associated with the ubiquitin–proteasome complex, a large multicatalytic–protease complex that is able to remove misfolded proteins to maintain a healthy cellular environment (Lee and Goldberg, 1998). Inhibition of proteasome activity increases polyQ protein aggregation and toxicity in cultured cells (Orr, 2001). The abnormal protein conformation of NH$_2$-terminal htt may be responsible for its aberrant nuclear accumulation and interactions with other proteins, leading to altered gene expression and neuropathology in HD. In an attempt to develop a therapeutic strategy to inhibit the generation of toxic htt fragments, experiments to identify NH$_2$-terminal mutant htt fragments have uncovered caspase and calpain cleavage products (Kim et al., 2001; Gafni and Ellerby, 2002; Goffredo et al., 2002; Wellington et al., 2002). Other NH$_2$-terminal fragments of mutant htt generated by unknown proteases were also identified in cultured cells (Lunkes et al., 2002; Sun et al., 2002). However, how these fragments are associated with neuropathology and whether they form nuclear inclusions in HD brain cells remain unclear.

The difficulty in defining toxic NH$_2$-terminal htt fragments in the brain stems from the inherent protein misfolding conferred by polyQ expansion. The polyQ-mediated conformational change results in unpredictable immunoreactivity and altered protein mobility on SDS gels, thereby making it difficult to identify the true size of NH$_2$-terminal htt fragments in the brain. In addition, postmortem HD brains are often poorly preserved, so their unknown integrity imposes additional difficulty in analyzing htt proteins.

Address correspondence to Xiao-Jiang Li, Dept. of Human Genetics, Emory University School of Medicine, 615 Michael St., Atlanta, GA 30322. Tel.: (404) 727-3290. Fax: (404) 727-3949.
email: xiaoli@genetics.emory.edu
Key words: Huntington's disease; polyglutamine; proteolysis; aging; aggregates

Figure 1. **Immunoreactivity of anti-htt antibodies.** (A) The regions of NH$_2$-terminal htt that were used for generating antibodies. 1C2 reacts with an expanded polyQ tract (triangle). (B) Western blot analysis of transfected htt with antibodies 1C2, EM48, 2166, and EM121. NH$_2$-terminal htt (1–508 aa) containing a 23 (23Q)– or 120 (120Q)– glutamine repeat was expressed in HEK293 cells that had been transfected for 72 h. NH$_2$-terminal htt fragments containing the expanded 120Q domain are marked with asterisks. Arrow indicates aggregated htt. Control, nontransfected cells. (C) Immunofluorescence double labeling of N508-120Q–transfected HEK293 cells with 2166 and EM48 (top) or EM121 with mouse antibody mEM48 (bottom). Arrows indicate cytoplasmic htt aggregates. (D) Immunostaining of the striatum of a homozygous HdhCAG150 mouse at 9 mo old with 1C2, 2166, EM121, and EM48. Only EM48 immunoreactive aggregates were seen. Bars: (C and D) 5 μm.
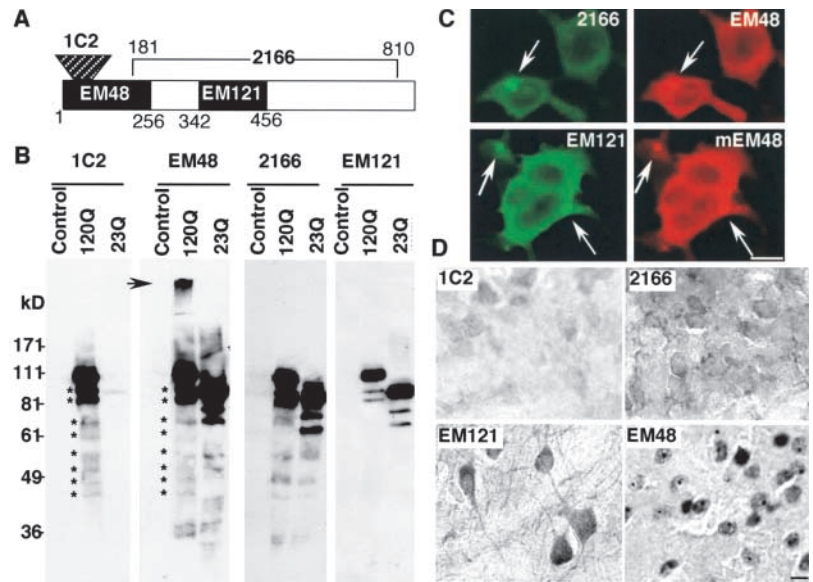
To circumvent these difficulties, we used several criteria to identify NH$_2$-terminal htt fragments that are genuinely toxic and likely to be associated with HD. First, toxic NH$_2$-terminal htt fragments must carry an expanded polyQ repeat and should be found specifically in the HD brain. Second, toxic NH$_2$-terminal htt fragments should be able to accumulate in the nucleus and form inclusions. Third, the accumulation of toxic NH$_2$-terminal htt fragments should be associated with disease progression. We used HD repeat knockin mouse brains, which allow observation of the initial formation of NH$_2$-terminal htt and its aggregates. Here, we provide evidence that the complex NH$_2$-terminal mutant htt fragments accumulate in the nucleus and form aggregates in association with the age-dependent decrease of proteasome activity. These results suggest that removing these toxic NH$_2$-terminal htt fragments may be an effective therapy to prevent htt toxicity.

Results

Immunoreactivity of anti-htt antibodies

Using human embryonic kidney 293 (HEK293) cells transfected with the first 508 aa of htt containing 23 (N508-23Q)– or 120 (N508-120Q)–glutamine repeats, we compared the immunoreactivity of some of widely used antibodies. These antibodies included EM48, a rabbit antibody against the first 256 aa of htt with a deletion of the polyQ domain (Gutekunst et al., 1999); 1C2, a mouse mAb against expanded polyQ tracts (Lunkes et al., 2002); and 2166, a mouse mAb against htt amino acids 181–810 (Dyer and McMurray, 2001). We also generated a rabbit antibody (EM121) that reacts with human htt amino acids 342–456 (Fig. 1 A). All these antibodies reacted with the intact form (∼110 kD) of N508-120Q (Fig. 1 B). When cells were transfected for 72 h, 1C2, EM48, and 2166 recognized many small bands ranging from 40 to 90 kD in N508-120Q cells. Among them, 1C2 immunoreactive bands certainly represent NH$_2$-terminal mutant htt fragments containing an expanded polyQ domain, as 1C2

failed to detect any bands of transfected htt containing a normal repeat (N508-23Q). The bands corresponding to 1C2 immunoreactive products were also seen on the EM48-probed blot (Fig. 1 B, arrowhead). Antibody 2166 labeled the same small bands that were present in both N508-120Q and N508-23Q samples, suggesting that these bands do not contain an expanded polyQ domain. EM121 did not label bands <80 kD in N508-120Q samples. Thus, small sized bands (<80 kD) labeled by both EM48 and 1C2 are likely to be NH$_2$-terminal mutant htt fragments smaller than the first 342 aa of htt. However, 1C2 did not label aggregated htt in the stacking gel. In contrast, EM48 intensely reacted with the aggregated htt on Western blots.

We also compared the immunoreactivity of these antibodies by immunocytochemistry. Overexpressed N508-120Q formed a few cytoplasmic aggregates in HEK293 cells, which were labeled by 2166, EM121, and EM48 (Fig. 1 C). This result suggests that polyQ aggregation did not mask the epitopes for 2166 and EM121. Immunostaining of HdhCAG150 mouse brains, however, only showed EM48-immunoreactive aggregates in the nucleus (Fig. 1 D). This result suggests that the brain aggregates do not contain epitopes that are recognizable by 2166 and EM121, or are formed by htt fragments smaller than the first 342 aa. 1C2 failed to detect htt aggregates in transfected cells (not depicted) and in HD brain (Fig. 1 D). The comparison of these antibodies indicates that 1C2 is particularly useful to detect the soluble form of mutant htt, whereas EM48 is the most sensitive to aggregated htt.

Composition of htt aggregates in brains of HD patients

Next, we examined htt aggregates in the caudate brain region from an HD patient with grade 3 neuropathology. Double immunofluorescence staining only showed EM48-labeled htt aggregates, which were negative to 1C2, 2166, and EM121 labeling (Fig. 2 A). This result also suggests that htt aggregates in the human brain primarily consist of small NH$_2$-terminal htt fragments.
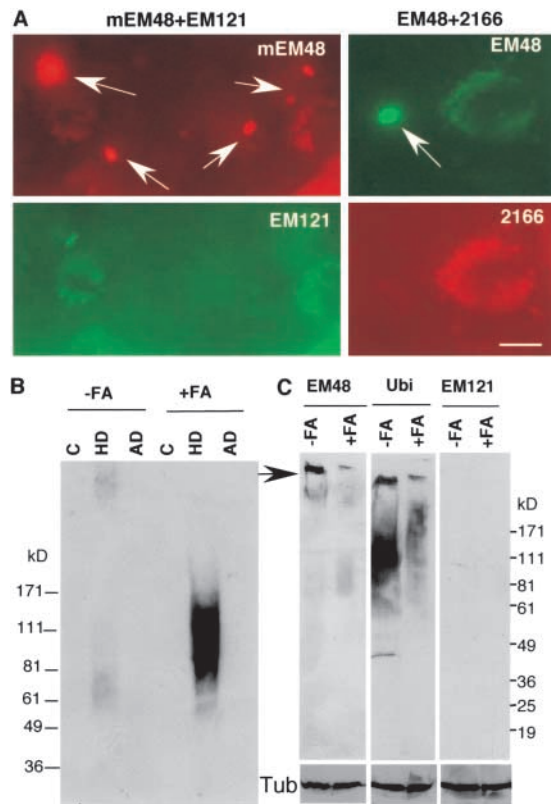
Figure 2.   **Aggregated NH$_2$-terminal htt in the cortex of HD patient brains.** (A) Double immunofluorescence labeling of a striatal section of an HD patient brain with mouse EM48 (mEM48) and EM121 or rabbit EM48 and 2166. Only EM48 reacted with htt aggregates in the brain. Arrows indicate htt aggregates. Bar, 5 μm. (B) The nuclear fractions of the striatum from control (C), HD, and Alzheimer's disease (AD) were dissolved with formic acid (FA) and resolved by SDS-PAGE. Products immunoreactive to 1C2 were not seen without FA treatment (−FA) but appeared as a smear in the HD sample after FA treatment (+FA). (C) FA treatment reduced the amount of EM48 or ubiquitin-labeled aggregates (arrow). EM48 and antiubiquitin reacted weakly with dissolved htt aggregates. EM121 did not label aggregated or dissolved htt. The blots were also probed with antibody against tubulin (Tub).

Figure 3.   **Complex NH$_2$-terminal htt fragments formed in HdhCAG150 mice.** (A) Homogenates of brain cortex from wild-type and heterozygous HdhCAG150 mice at 3, 6, 10, and 18 mo old were analyzed by Western blotting with EM121 or 1C2. Note that no 1C2 immunoreactive products were seen in the wild-type (WT) mouse brain. In vitro–synthesized N508-120Q was included to estimate the size of htt in the brain. (B) Extracts of various brain regions (Str, striatum; Cereb, cerebellum; and Ctx, cortex) from heterozygous HdhCAG150 mice at different ages (2, 6, and 12 wk, or 16 mo) were analyzed by Western blotting with 1C2. Arrow indicates full-length mutant htt. (C) Cytoplasmic and nuclear fractions of HD mice at the age of 3, 5, or 12 wk were analyzed by 1C2 Western blotting. Arrow indicates full-length htt. (D) Nuclear aggregates isolated from HD mouse cortex were treated with FA and analyzed by Western blots with 1C2 antibody. Note that distinct 1C2 immunoreactive products were present in dissolved aggregates from 3-mo-old HD mice and became a smear over time. The brackets in B–D show multiple NH$_2$-terminal htt fragments that are smaller than N508-120Q. The blots were also probed with antibodies against tubulin (Tub) or the neuron-specific nuclear protein NeuN.

Several studies have shown that the homogenates of postmortem brains of HD patients display a smear of 1C2 immunoreactive products on Western blots (Kim et al., 2001; Lunkes et al., 2002; Wellington et al., 2002). However, the composition of nuclear htt inclusions in the brain is unclear. Therefore, we isolated htt inclusions from the brains of HD patients and dissolved them with formic acid. A very intense 1C2 smear was seen in the dissolved aggregates (Fig. 2 B). Although EM48 and antiubiquitin antibodies labeled aggregated proteins, these antibodies reacted weakly with dissolved htt (Fig. 2 C), suggesting that dissolved mutant htt possesses a different conformation that is more recognizable by 1C2. EM121 did not recognize htt aggregates or their dissolved products (Fig. 2 C).

Multiple NH$_2$-terminal htt fragments in HD mouse brain

The smear of 1C2 immunoreactive products in the HD brain sample may result from htt oligomerization or conjugation with other molecules over time in the human
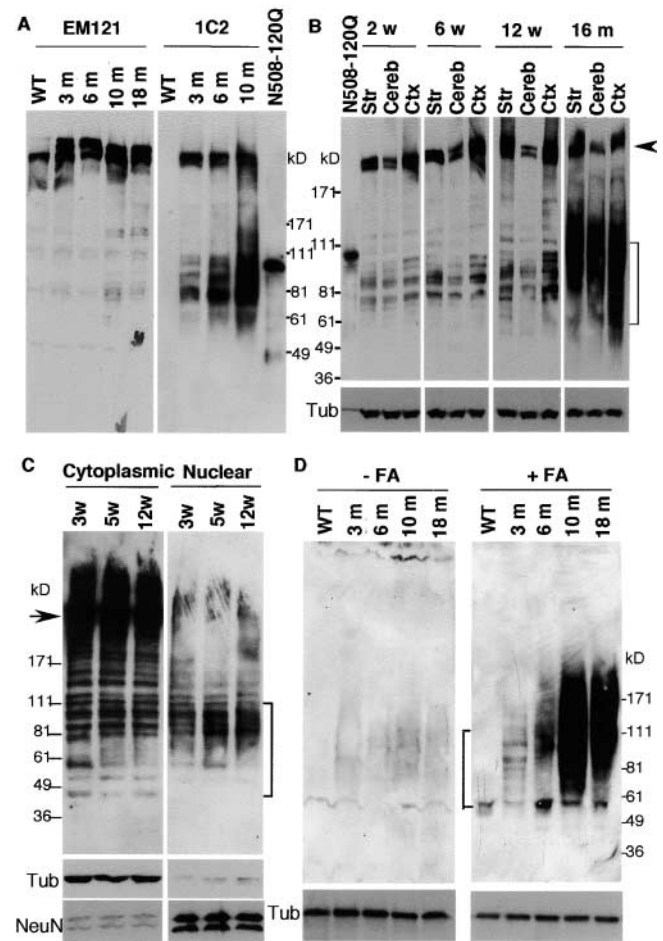
brain, precluding any analysis of the size of htt fragments. Therefore, we examined HD repeat knockin mice (HdhCAG150), which express a 150–glutamine repeat in endogenous mouse htt (Lin et al., 2001). These mice show progressive neurological symptoms beginning at the age of 4–5 mo (Lin et al., 2001). Using EM121, we found that the mutant and normal alleles were expressed at equivalent levels from 3 to 18 mo (Fig. 3 A). Products immunoreactive to 1C2 were seen only in the HD mouse brain, again support-

ing the idea that they are NH$_2$-terminal mutant htt. Strikingly, small 1C2 immunoreactive bands became prominent with increasing age, reflecting the accumulation of NH$_2$-terminal mutant htt in old animals (Fig. 3 A). In vitro–synthesized N508-120Q was then included to estimate the size of the NH$_2$-terminal htt fragments in the HD brain. Because mutant htt in HD mice contains a longer repeat (150Q), 1C2-labeled bands that were smaller than N508-120Q (110 kD) certainly represent htt fragments shorter than the first 508 aa of htt. To further examine whether these fragments were generated in young HD mice (<3 mo), we isolated various brain regions from 2 wk–16-mo-old HD mice and found that multiple 1C2 immunoreactive bands were also present in these regions. Noticeably, the amount of these 1C2 bands was less in the cerebellum than in the striatum and cortex, perhaps because of the low level of full-length mutant htt in this brain region. A more strikingly finding is that these NH$_2$-terminal htt fragments were generated even at the age of 2 wk (Fig. 3 B). This clearly indicates that the generation of multiple NH$_2$-terminal htt fragments precedes any detectable neurological symptoms, as HdhCAG150 mice usually exhibit neurological phenotypes at the age of 5–6 mo (Lin et al., 2001).

It would be interesting to know whether these NH$_2$-terminal htt fragments are also present in the nucleus. Next, we compared 1C2 immunoreactive products in cytosolic and nuclear fractions of the cortex of HD mice at the age of 3–12 wk. With a longer exposure of Western blots, multiple htt fragments were obviously seen in these samples (Fig. 3 C). Most htt fragments seen in the nuclear fraction were <110 kD (Fig. 3 C, bracket), suggesting that these smaller fragments were prone to nuclear accumulation.

Next, we isolated nuclear htt aggregates from HD mouse brains and dissolved them using formic acid. Several distinct bands were observed in the dissolved htt aggregates. However, these bands were distinguishable only in young mice at the age of 3 mo and, as the age increased (from 6 to 18 mo), they became a smear resembling the smear seen on Western blots of the brain of HD patients. In addition, the bands in older mouse brains appeared to be larger, owing to the oligomerization or conjugation of intranuclear htt in aged neurons (Fig. 3 D). Thus, nuclear htt inclusions may be initially formed by multiple NH$_2$-terminal htt fragments (smaller than the first 508 aa), which then become oligomerized or aggregated in an age-dependent manner.

Cleavage of small NH$_2$-terminal htt fragments

Complex NH$_2$-terminal htt fragments seen in the HD mouse brain reflect multiple cleavage products of htt. To examine whether mouse brain extracts could also cleave NH$_2$-terminal htt to small fragments in vitro, we used an in vitro cleavage method as described previously (Kim et al., 2001; Wellington et al., 2002) to examine how the in vitro–synthesized N508-120Q is digested by mouse brain extracts. The experiment included mouse brain extracts of the cortex, cerebellum, striatum, hippocampus, and brain stem. Multiple fragments were observed after the in vitro digestion by these tissue extracts. However, no tissue-specific band was observed under these conditions (Fig. 4 A). Inclusion of N508-23Q verified that these htt products
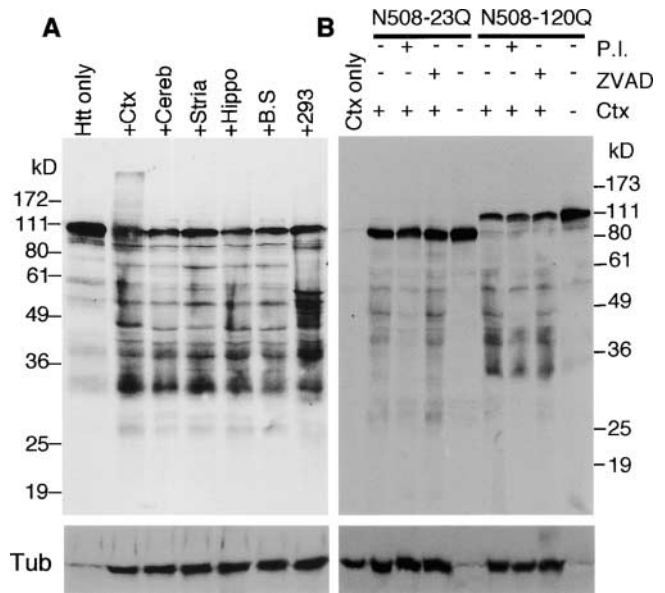

Figure 4. **Lack of caspase cleavage of NH$_2$-terminal htt.** (A) In vitro–synthesized htt (N508-120Q) was digested by 100 µg protein extracts of various mouse brain regions (Ctx, cortex; Cereb, cerebellum; Stria, striatum; Hippo, hippocampus; B.S, brain stem; and 293, HEK293 cell lysates). Degraded htt products were revealed by mEM48 Western blotting. (B) Fragments of N508-23Q and N508-120Q that were cleaved by mouse cortex extracts showed repeat-dependent mobility on a Western blot. Some of these fragments were inhibited by a mix of protease inhibitors (P.I.) but not by 50 µM of caspase inhibitor (ZVAD). Cortex extract alone (Ctx only) served as a control to verify that the mEM48-labeled products were specifically derived from the in vitro–synthesized htt. Probing the blots with antitubulin (Tub) showed that the equal amounts of brain lysates were used.

did contain a polyQ domain (Fig. 4 B), as evidenced by the repeat length–dependent migration of these bands on the SDS gel. When incubated with a mix of protease inhibitors, some of these NH$_2$-terminal htt fragments were significantly inhibited. A caspase inhibitor (ZVAD), which inhibits a variety of caspases, did not affect these htt fragments, perhaps because caspase cleavage occurs at positions at and beyond amino acid 513 (Kim et al., 2001; Wellington et al., 2002).

Multiple NH$_2$-terminal htt fragments in stably transfected cells expressing full-length mutant htt

To confirm that complex NH$_2$-terminal htt fragments are generated from full-length mutant htt, we established stably transfected HEK293 cells (23Q-F or 120Q-F) that express full-length htt containing a 23Q or 120Q repeat. Immunostaining of 120Q-F cells showed that these cells formed htt aggregates only when they had been cultured for 3–4 d (Fig. 5 A). Because only NH$_2$-terminal mutant htt forms aggregates, Western blots were performed to examine the generation of NH$_2$-terminal htt in these cells. Compared with 23Q-F cells, 120Q-F cells clearly showed more NH$_2$-terminal mutant htt fragments that were intensely labeled by EM48 (Fig. 5 B). Their amount increased after culturing for 3–4 d. Also, the size of these fragments ranged from 55 to 98 kD, consistent with the idea that they are smaller than the first 500 aa of htt.
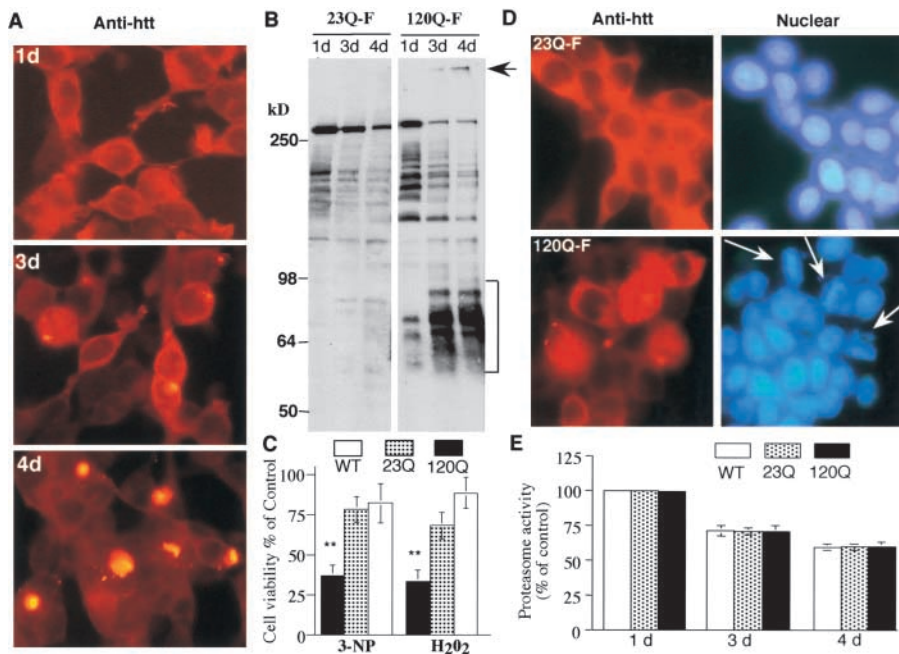
Figure 5. **Toxic NH$_2$-terminal htt fragments in full-length mutant htt-transfected cells.** (A) HEK293 cells stably transfected with full-length htt containing a 120 (120Q-F)–glutamine repeat displayed EM48-labeled aggregates in 3–4-d-old cultured cells. (B) Western blot analysis of 120Q-F and 23Q-F cells showing that EM48 immunoreactive fragments smaller than the first 500 aa of htt (bracket) were accumulated in cultured cells at days 3–4. Arrow indicates full-length htt. (C) A greater decrease in the viability of 120Q-F cells was observed after treatment with 5 mM of oxidative insults 3-NP and 200 μM of hydrogen peroxide for overnight. Control is cells without drug treatment. The data (mean ± SD) were expressed as percentage of control. ANOVA and posthoc Scheffe's test confirmed a statistical difference between 120Q-F and 23Q-F cells or nontransfected cells.**, indicates P < 0.0003; F > 30.71; and n = 4. (D) Representative images of 23Q-F or 120Q-F cells treated with 10 mM 3-NP overnight. Cells were stained with anti-htt (mEM48) antibody and the nuclear dye Hoechst. Arrows indicate fragmented nuclei. (E) Proteasome activity of cultured cells was decreased after prolonged culture (3–4 d). The data are expressed as mean ± SD (n = 3). The proteasome activity of WT cells at day 1 is presented as 100%. Error bars represent mean ± SD.

The viability of 23Q-F and 120Q-F cells did not differ significantly under normal culture conditions (unpublished data), perhaps because htt toxicity is dependent on the accumulation of cleaved NH$_2$-terminal htt fragments. It is possible that mutant htt in these cells mediates early pathological events or confers cellular vulnerability to certain insults. Thus, we treated these cells with the mitochondrial toxin 3-nitropropionic acid (3-NP), which has been used to establish HD animal models (Beal et al., 1993). Using modified 3-(4,5-dimethyl thiazol-2-yl)-2,5-diphenyl tetrazolium bromide (MTS) assay that detects early apoptotic events, we found that 3-NP significantly reduced the viability of cells carrying 120Q-F (36.8% ± 6.4) as compared with 23Q-F cells (78.3% ± 8.2) and nontransfected cells (82.1% ± 12.3). Hydrogen peroxide, another oxidative stress insult, also caused a significant decrease in the viability of 120Q-F cells (33.3% ± 7.2) relative to 23Q-F (68.1% ± 8.3) and control cells (88.5% ± 9.8; Fig. 5 C, n = 4). The MTS assay has been widely used to measure cell viability, as it is able to detect the function of dehydrogenases and thus, measures mitochondrial dysfunction during early stages of cell death. However, this dysfunction may not always reflect apoptotic events. Although no significant morphological changes were seen in 120Q-F cells under the normal culturing conditions, we wanted to know whether 3-NP treatment could lead these cells to have nuclear fragmentation that reflects cell death. By examining the nuclear morphology of cultured cells, we found that more 120Q-F cells (15.25% ± 1.75 [mean ± SEM]) had obvious abnormal or fragmented nuclei than did 23Q-F cells (7.25 ± 1.25) and nontransfected cells (4.5% ± 0.64; Fig. 5 D). Analysis of variance (ANOVA) and posthoc Scheffe's test showed significant differences between 120Q-F cells and nontransfected cells

(P = 0.0011; F = 33.21; and n = 4) or 23Q-F cells (P = 0.0098; F = 13.8; and n = 4). Considering the increased generation of htt fragments in these 120Q-F cells, these results suggest the association of NH$_2$-terminal htt fragments with increased sensitivity to oxidative toxins. The increased levels of NH$_2$-terminal mutant htt could result from the decreased ability to remove these fragments. Because proteasome activity in cultured cells often decreases after prolonged culturing (Starke-Reed and Oliver, 1989; Dardevet et al., 1995; Petropoulos et al., 2000; Bulteau et al., 2000), we examined proteasome activity of cultured cells and found a lower activity in old cultured cells, including wild-type, 23Q-F, and 120Q-F cells (Fig. 5 E). This decrease apparently paralleled the increased amount of NH$_2$-terminal htt in 120Q-F cells, suggesting that decreased proteasome activity promotes the accumulation of NH$_2$-terminal mutant htt.

Age-dependent decrease in brain proteasome activity

The inverse correlation between decreased proteasome activity and increased accumulation of NH$_2$-terminal htt in 120Q-F cells led us to examine whether proteasome activity also decreases in aged HD neurons, which contain more NH$_2$-terminal htt fragments. Because small NH$_2$-terminal htt accumulates in the nucleus, we first examined the nuclear distribution of htt in HdhCAG150 mouse brains. In the striatum, nuclear htt staining was evident at 3 mo old. As the mice aged, intranuclear htt staining became more intense and formed nuclear aggregates (Fig. 6 A). These results are consistent with Western blot results showing that more NH$_2$-terminal htt fragments accumulated in older HD mouse brains (Fig. 3 A). We also observed many htt aggregates in the cortex in HdhCAG150 mice (unpublished data), perhaps because a large repeat (150Q) reduces the tis-
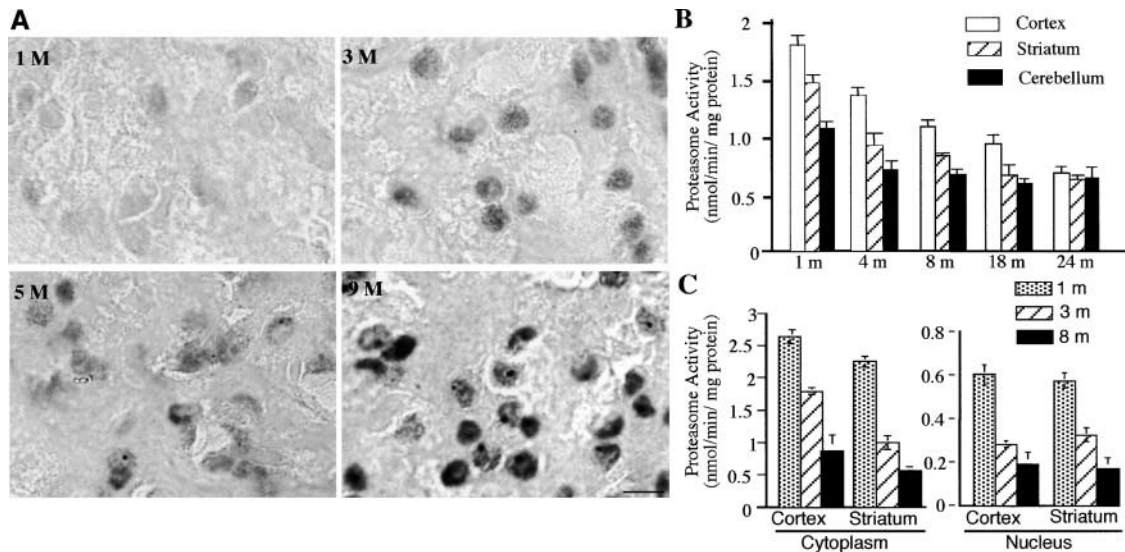
Figure 6. **Age-dependent decrease of proteasome activity and increase in nuclear accumulation of mutant htt.** (A) The striatal region from homozygous HdhCAG150 mice at 1, 3, 5, and 9 mo old was stained with EM48. Htt aggregates increased with the age of the brain. Bar, 10 μm. (B) Chymotrypsin-like proteolysis was assayed in homogenates from various brain regions of 1–24-mo-old mice. Error bars represent mean ± SD. (C) The cytoplasmic and nuclear fractions of the cortical and striatal tissues were examined for chymotrypsin-like activity at various ages (1, 3, and 8 mo). Proteasome activity is expressed as nanomol/minute/milligram protein (mean ± SD; and $n = 3$–5 mice).

sue-specific distribution of polyQ protein, as reported in SCA1 mouse model (Watase et al., 2002). However, in the same animal, more intranuclear htt aggregates were often observed in the striatum than in the cortex.

Next, we measured the hydrolysis of Suc-Leu-Leu-Val-Tyr-4-methyl-coumaryl-7-amide (Suc-LLVY-MCA) by chymotrypsin-like proteasomes in brain homogenates from wild-type and HD mice at 1–24-mo old (Fig. 6 B). Three brain regions of these mice were examined: the cerebral cortex, the striatum, and the cerebellum. We did not see any significant difference in this proteasome activity between normal and HD mouse brains at various ages (unpublished data). However, all the brain tissues examined showed decreasing proteasome activity as the mice aged. The striatum showed the greatest reduction in activity from 1 to 4 mo. After 8 mo, the activity decreased steadily and slowly. Although chymotrypsin-like activity is lower in the nucleus than in the cytosolic lysates, nuclear proteasome activity also decreased in an age-dependent fashion (Fig. 6 C). The activity of postglutamyl peptidase, which uses Z-LLLE-βNap as a substrate and is also present in 20S proteasome (Piccinini et al., 2000), also decreased in the striatal cells (unpublished data). The significant decrease of proteasome activity from 1 to 3 mo is fairly consistent with the increased nuclear staining of htt and the increased accumulation of NH$_2$-terminal htt fragments in HdhCAG150 mice.

Accumulation of NH$_2$-terminal htt by inhibiting proteasome activity

If decreased proteasome activity causes the increased amount of NH$_2$-terminal htt, inhibiting proteasomes should also promote the accumulation of NH$_2$-terminal htt fragments. We performed three sets of experiments to test this hypothesis. First, HEK293 cells that had been transfected with N508-23Q or N508-120Q were treated with *N*-acetyl-

leucinal-leucinal-norleucinal (ALLN) and lactacystin, which are used to inhibit proteasomes in a variety of systems (Johnston et al., 1998; Lee and Goldberg, 1998). Transfection of cells for 24 h gave rise to a prominent band of intact transfected htt, but proteasome inhibition resulted in a significant increase in small NH$_2$-terminal htt fragments (Fig. 7 A). More NH$_2$-terminal htt products were present in N508-23Q cells than in N508-120Q cells after inhibiting proteasomes, perhaps because NH$_2$-terminal htt fragments containing 120Q were unstable and quickly became aggregates, especially when proteasomes are inhibited. Indeed, aggregated htt that remained in the stacking gel was labeled by EM48.

Our second experiment was to examine whether decreased proteasome activity in brain tissue could promote the accumulation of NH$_2$-terminal htt. To do so, we incubated the in vitro–synthesized NH$_2$-terminal htt (N508-120Q) with striatal extracts from mice at 1 or 3 mo old (Fig. 7 B). In the absence of protease inhibitors, the in vitro–synthesized htt had several degraded fragments, allowing us to examine their digestion by tissue proteasomes. It appeared that brain extracts from 1-mo-old mice removed more fragments than did the extracts from 3-mo-old mice, consistent with the higher proteasome activity in the younger animals. Inhibiting proteasomes by lactacystin restored these NH$_2$-terminal htt fragments. Furthermore, htt products were seen that were larger than the intact form of N508-120Q, especially when htt was treated with lactacystin and incubated with the older brain extracts. This result suggests that inhibiting proteasome activity also promotes the oligomerization or conjugation of NH$_2$-terminal mutant htt.

In our third experiment, we examined whether proteasome inhibition could increase the accumulation of endogenous NH$_2$-terminal mutant htt fragments in HD brain. After treating the nuclear extracts of HD mouse striatum with
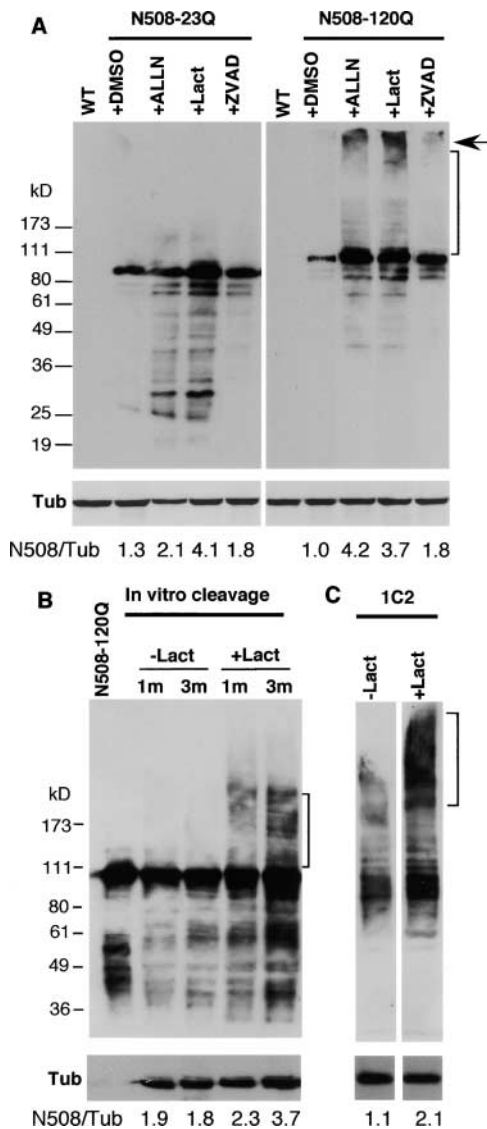
Figure 7.   **Effect of inhibiting proteasome activity on the accumulation of NH$_2$-terminal htt fragments.** (A) HEK293 cells transfected with N508-23Q or N508-120Q for 24 h were treated with vehicle (DMSO), 20 μg/ml ALLN, 20 μM lactacystin (Lact), or 50 μM ZVAD overnight. EM48 Western blots revealed multiple htt fragments, htt of high molecular mass (bracket), and aggregated htt (arrow) after ALLN and Lact treatment. (B) In vitro–synthesized N508-120Q was incubated with 100 μg protein of mouse striatal extracts in the absence (−Lac) or the presence (+Lac) of 20 μM lactacystin for 1 h. Note that 1-mo-old (1m) striatal extracts removed more 1C2 immunoreactive fragments than did the extracts from 3-mo-old (3m) mice. Inhibiting the proteasome by lactacystin increased the amount of NH$_2$-terminal htt products and their oligomerization or conjugation (bracket). Blots were also probed with antitubulin (bottom, Tub). (C) Striatal extracts from HdhCAG150 (+/+) mice at 4 wk old were treated with lactacystin (+Lac, 20 μM) for 1 h, resulting in more 1C2 immunoreactive fragments and htt of high molecular mass (bracket). Relative signal ratios of the intact form of N508 htt to tubulin (N508/Tub) are shown.

lactacystin, we also observed a significant increase in multiple 1C2 immunoreactive products and, more importantly, an increase in the oligomerized or aggregated htt of high molecular weight (Fig. 7 C). These oligomerized or aggregated htt proteins were not labeled by antiubiquitin anti-

body (unpublished data). It is likely that ubiquitination of aggregated htt requires time such that those htt aggregates that form rapidly in vitro or in transfected cells are often not ubiquitin immunoreactive.

Discussion

Given that NH$_2$-terminal htt fragments with an expanded polyQ domain are toxic to neurons, reducing their production or removing them would be beneficial for treating HD. However, effective inhibition of mutant htt degradation largely depends on the identification of htt fragments and their cleavage sites. Previous studies have focused on how mutant htt fragments are generated (DiFiglia et al., 1997; Kim et al., 2001; Mende-Mueller et al., 2001; Gafni and Ellerby, 2002; Lunkes et al., 2002; Wellington et al., 2002). As a result, various htt fragments were identified. However, the nature of toxic NH$_2$-terminal htt fragments in the HD brain is still poorly understood. This paper demonstrates that complex NH$_2$-terminal htt fragments are naturally generated in the HD brain before neurological symptoms and suggests that an age-dependent decrease in clearance of these fragments is important for the development of the disease.

A number of NH$_2$-terminal htt fragments of varying sizes have been found in the brains of HD patients (DiFiglia et al., 1997; Kim et al., 2001; Mende-Mueller et al., 2001). The variable integrity of postmortem brain tissues examined and the varied immunoreactivity of antibodies used may cause inconsistent results regarding the size of NH$_2$-terminal htt fragments. Another obstacle to analyzing NH$_2$-terminal htt fragments stems from unpredictable protein conformational changes caused by polyQ expansion. NH$_2$-terminal htt fragments, once generated from full-length htt, may be unstable or possess varied immunoreactive properties. For example, although EM48 reacts well with NH$_2$-terminal htt fragments in transfected cells, it is poor in recognizing brain NH$_2$-terminal htt fragments on blots. This may explain why very few NH$_2$-terminal htt fragments have been found in HD mouse brains with EM48 Western blots (Li et al., 2000; Wheeler et al., 2000). NH$_2$-terminal mutant htt might be either rapidly degraded by the proteasome or become misfolded and aggregated to form visible inclusions. Indeed, reducing polyQ oligomerization was found to promote the degradation of polyQ proteins and to inhibit their toxicity (Sanchez et al., 2003). It remains to be investigated how soluble mutant htt forms aggregates. However, it is possible that protein conformational changes caused by polyQ expansion create an epitope that is more recognizable by 1C2 on Western blots, and such an epitope is lost or masked during polyQ aggregation such that 1C2 is unable to react with aggregated htt. This explains why 1C2 fails to detect distinct NH$_2$-terminal htt fragments in aged patient brains (Dyer and McMurray, 2001) but often recognizes a smear after dissolving aggregated htt (Lunkes et al., 2002; Wellington et al., 2002). Thus, HD mice at young ages would provide a better system to uncover NH$_2$-terminal htt fragments that have not been aggregated. Also, the HD mice we examined express a 150–glutamine repeat. This large repeat significantly increased 1C2 immunoreactivity, allowing us to reveal more NH$_2$-terminal htt fragments than reported previously.

Proteins identified by 1C2 in this paper certainly represent toxic NH$_2$-terminal htt fragments in the brain. First, their formation precedes disease symptoms, and their increased accumulation is well correlated with disease progression. Second, unlike full-length mutant htt, small 1C2 immunoreactive products accumulate in the nucleus, indicating that they are translocated into the nucleus and may affect gene expression. Third, oligomerization of polyQ proteins is toxic to cells (Sanchez et al., 2003). Small 1C2 immunoreactive products are oligomerized and aggregated. In support of this, dissolving nuclear inclusions revealed a similar complex of 1C2 immunoreactive products. Fourth, the generation of similar NH$_2$-terminal htt fragments in transfected cells is closely associated with the increased vulnerability to oxidative toxins. Furthermore, the cytotoxicity of small NH$_2$-terminal htt fragments has been convincingly demonstrated in HD transgenic mice (Davies et al., 1997; Schilling et al., 1999).

Some of the NH$_2$-terminal htt fragments observed in our work might be generated from the identified cleavage sites by caspase-3, calpain, and an unknown aspartic endopeptidase (Gafni and Ellerby, 2002; Kim et al., 2001; Lunkes et al., 2002; Wellington et al., 2002). However, the repeat-dependent mobility on the blots makes it difficult to compare the size of NH$_2$-terminal htt fragments we observed with that of different htt or different polyQ repeats in other studies. Despite this, it is evident that multiple NH$_2$-terminal htt fragments are present in very young animals, suggesting that various proteases are actively producing these fragments throughout the animal's lifetime.

The concentration of specific NH$_2$-terminal htt fragments is determined by their rates of generation and degradation. Examination of several brain regions did not reveal any tissue-specific 1C2 immunoreactive fragment. We cannot rule out the possibility that tissue-specific htt products are unstable or rapidly subjected to further modification or digestion. This paper shows that further degradation of multiple NH$_2$-terminal htt products plays a critical role in their turnover. Although chaperones prevent misfolding of proteins, the ubiquitin–proteasome systems degrade small polyQ peptides or misfolded proteins (Orr, 2001). The proteasome is a large multicatalytic–protease complex, which exists as 20S ($\sim$700 kD) and 26S ($\sim$2,000 kD) particles (Coux et al., 1996). The 20S particle, the catalytic core of the proteasome, is composed of 14 discrete but related subunits. A recent paper using oligonucleotide assays shows that the ubiquitin–proteasome pathway is suppressed at the transcriptional level in the aged brain (Lee et al., 2000). Proteasome activity was also found to decrease in the aged rat brain (Keller et al., 2000). We observed similar decreased activity of both chymotrypsin-like proteasomes and postglutamyl peptidase in the striatum, which is particularly vulnerable in HD (Vonsattel et al., 1985). Thus, the age-dependent decrease in proteasome activity may reduce the clearance of degraded htt and contribute to the progressive accumulation of NH$_2$-terminal mutant htt fragments. Consistent with this idea, proteasome inhibition results in the accumulation of HD exon 1 protein in transfected cells (Waelter et al., 2001) and other NH$_2$-terminal htt fragments generated in NG108 cells (Lunkes et al., 2002). However, this paper shows that multiple mutant htt NH$_2$-terminal fragments were generated in HEK293 cells after inhibiting the proteasomes promotes. More importantly, the generation of multiple mutant NH$_2$-terminal htt fragments naturally occurs in mouse brain and is also increased by proteasome inhibition.

Because proteasome activity also decreases in various tissues in aged animals, its age-dependent decrease is unlikely to critically contribute to the specific neuropathology in HD. The selective neuropathology of HD may be dependent on the sensitivity of neurons to toxic htt fragments, whereas the age-dependent decrease in neuronal proteasome activity is more likely to promote the disease process mediated by misfolded proteins.

Recent studies show that polyQ inclusions sequester proteasomes and reduce proteasome activity in cultured cells (Bence et al., 2001). It is possible that aggregated htt may affect proteasome function when it forms large inclusions or when cells are under stress. The presence of fewer htt inclusions in our cell lines might not allow us to observe the effect of htt inclusions on proteasome activity. Similarly, we did not find that brain proteasome activity is specifically altered in HD repeat knockin mouse brain as compared with age-matched wild-type mice. Rather, we observed that neuronal proteasome activity is decreased over time and that this age-dependent decrease is associated with the accumulation of NH$_2$-terminal htt fragments and their aggregation.

Our study also suggests that proteolysis of mutant htt does not bear analogy to that of the amyloid protein, whose cleavage by a few defined secretases produces distinct toxic fragments in Alzheimer's disease (Esler and Wolfe, 2001). PolyQ proteins may be more accessible to a number of proteases and further degradation by the ubiquitin–proteasome systems. This paper suggests that improving and restoring a cell's ability to clear toxic protein fragments would be a more effective route to reducing the toxicity of NH$_2$-terminal htt fragments. Martin-Aparicio et al. (2001) demonstrated that proteasome inhibition can abolish the reversal of the expression and aggregation of mutant htt in HD mice, which also suggested that decline in proteasome activity plays a role in late onset pathology. Given the critical role of the proteasome in removing toxic and misfolded proteins and the age-dependent decrease in its activity, drugs and chemicals that improve the function of the proteasome in aged neurons may provide effective intervention to slow or prevent the progression of HD and other age-dependent neurodegenerative diseases in which toxic proteins are misfolded.

Materials and methods

HD mice and postmortem brains of HD patients

HdhCAG150 mice, which express a 150-CAG repeat in the endogenous mouse HD gene, were generated previously and provided by P. Detloff (University of Alabama at Birmingham, Birmingham, AL) (Lin et al., 2001). These HD mice were maintained in the animal facility at Emory University. Brain tissues from HdhCAG150 mice at various ages were used for analysis.

Frozen human brain tissues from pathologically normal individuals, Alzheimer's disease, and HD patients were provided by the Harvard Brain Tissue Resource Center. The caudate brain region was obtained from five HD patients aged from 39 to 75, and the postmortem interval was between 12 and 27 h. The pathological severity of these brains is grade 3 based on published criteria (Vonsattel et al., 1985). Expanded CAG repeats (41–47 U) in these HD brains were confirmed by PCR of brain genomic DNA using an established method (Mende-Mueller et al., 2001).

Antibodies

EM48, a rabbit pAb against the NH$_2$-terminal region (amino acids 1–256) of human htt, was generated from our previous paper (Gutekunst et al., 1999). Mouse mAb mEM48 was generated using the same antigen as for the rabbit EM48 (Li et al., 2002). EM121 was a rabbit antibody generated using GST-HD2 fusion proteins containing amino acids 342–456 of human htt (Covance, Inc.). Mouse mAbs to γ-tubulin (Sigma-Aldrich), htt (2166 and 1C2; CHEMICON International, Inc.), and neuron-specific nuclear protein NeuN (CHEMICON International, Inc.) were also used.

cDNA constructs and transfection of cells

pEBVHis (Invitrogen) expression constructs containing full-length human htt with 23 (23Q-F) or 120 (120Q-F) glutamines in the repeat were transfected into HEK293 cells. We selected stable transfected htt cells with 500 ng/ml of the antibiotic hygromycin and obtained four independent lines of 120Q-F and six lines of 23Q-F. HEK293 cells were originally obtained from American Type Culture Collection and were used to generate stably transfected cells. The 120Q-F-1 and 23Q-F-5 cell lines were used for further analysis. Htt cDNAs containing the first 508 aa with 23 (N508-23Q) or 120 (N508-120Q) glutamines were obtained from our previous paper (Gutekunst et al., 1999) and used for transfection of HEK293 cells.

Western blots, fractionation, and light microscopic examination

Homogenates of brain tissue and cultured cells were resuspended in PBS with protease inhibitor cocktail (1× P8340; Sigma-Aldrich), 100 µg/ml PMSF, and 1% Triton X-100. Western blotting was performed using 4–12% or 4–20% polyacrylamide Tris-Glycine gels (Invitrogen) and ECL kits (Amersham Biosciences).

To isolate the nuclear fraction, brain tissue was homogenized in buffer (0.25 M sucrose, 15 mM Tris-HCl, pH 7.9, 60 mM KCL, 15 mM NaCl, 5 mM EDTA, 1 mM EGTA, and 100 µg/ml PMSF). The homogenate was spun at 1,000 g for 15 min at 4°C. The cytosolic fraction was further isolated by centrifuging at 20,000 g for 15 min. The nuclear pellet was washed and resuspended in 1% SDS and spun down again at 20,000 g for 15 min. SDS resistant aggregates were isolated as described previously (Hazeki et al., 2002). They were washed twice with 60 mM Tris-HCl, pH 7.6, and precipitated by centrifugation at 20,000 g for 15 min. To dissolve htt aggregates, we treated the precipitated aggregates with 100% formic acid at 37°C for 30 min. The sample was resuspended in 0.1% SDS and dried under vacuum. The dried material was resuspended in 400 µl H$_2$O and precipitated with methanol/chloroform (Wessel and Flugge, 1984). The precipitated proteins were analyzed by Western blotting.

Immunostaining of brain sections and cultured cells was performed as described previously (Li et al., 2000, 2002). Light microscopic graphs of brain sections were taken at a magnification of 400 using a microscope (model Axioskop 2; Carl Zeiss MicroImaging, Inc.) connected with a Spot-RT digital camera (Diagnostic Instruments). Immunofluorescent images of samples, which were stained with secondary antibodies conjugated with either FITC or rhodamine (Jackson ImmunoResearch Laboratories), were taken using an inverted fluorescent microscope (model Axiovert 135; Carl Zeiss MicroImaging, Inc.) and video system (Dage-MTI Inc.) at a magnification of 400. The captured images were stored and processed using Adobe Photoshop software. To examine morphological changes of cultured cells, htt-transfected cells were cultured for 3 d in the normal medium, incubated with serum-free medium for 12 h, and treated with 10 mM 3-NP overnight. The cells were fixed, stained with mEM48 and Hoechst, and remained in PBS for examination with fluorescent microscopy at room temperature. Cells showing abnormal nuclear morphology or fragmentation were counted to obtain the percentage of dead cells. The data were obtained from four independent 3-NP treatments by examining 271–689-transfected cells for each group.

Cell viability assays

Cell viability was determined by a modified MTS assay (Cell Titer 96; Promega) with a microplate reader (SPECTRAmax Plus; Molecular Devices) as described previously (Li et al., 1999). For drug treatment experiments, cultured cells were treated with 5 mM 3-NP or 200 µM hydrogen peroxide for 12 h and examined with the MTS assay.

In vitro degradation of htt

In vitro–translated htt was obtained from PRK-htt constructs encoding the first 508 aa of htt using the TNT in vitro translation kit (Promega). Mouse tissues were homogenized in five volumes of PBS. The low speed (1,000 g) supernatant (100 µg protein /30 µl) was used for incubation (37°C for 1 h) with 2 µl of the in vitro–synthesized htt followed by termination with SDS sample buffer. To inhibit the in vitro cleavage of htt, 50 µM caspase inhib-

itor ZVAD (Enzyme Systems), protease inhibitor mix (consisting of pepstatin A, leupeptin, and chymostatin at 10 µM each, E64 and PMSF at 1 µM each in 1× P8340; Sigma-Aldrich), or 20 µg/ml proteasome inhibitor ALLN or 20 µM lactacystin (Qbiogene) was preincubated with tissue extracts for 45 min at 37°C. In vitro–synthesized htt without protease inhibitors showed multiple fragments and was used for further digestion by mouse brain extracts. Degraded products of htt were analyzed by Western blotting with 1C2 or mEM48. Densitometry was used to obtain relative ratios of the intact form of N508 htt to tubulin.

Proteasome activity assay

A fluorogenic peptide substrate assay for proteasome activity was performed as described previously (Figueiredo-Pereira et al., 1994; Canu et al., 2000). Brain tissues and cultured cells were homogenized in lysis buffer (10 mM Tris-HCl, pH 7.5, 1 mM EDTA, 2 mM ATP, 20% glycerol, and 4 mM DTT). The homogenate was centrifuged at 14,000 g at 4°C for 30 min. 20 µg of cell lysate proteins or 40 µg of nuclear proteins were incubated with 0.4 ml of proteasome activity assay buffer (50 mM Tris-HCl, pH 8.0, 1 mM EDTA, 1 mM ATP, and 40 µM Suc-LLVY-MCA; Qbiogene). The assay monitored the hydrolysis of the fluorogenic substrate, Suc-LLVY-MCA, into 7-amino-4-methyl-coumarin. To examine postglutamyl peptidase activity, we used 400 µM N-CBZ-Leu-Leu-Leu-Glu–β-naphthylamide (Sigma-Aldrich). A linear correlation between the proteasome activity and the reaction time was obtained at various times (15, 30, 45, 60, and 120 min). The reactions were stopped by adding 0.8 ml of cold water and incubating on ice for 10 min. The fluorescent intensity of each reaction was measured by fluorescence spectrophotometry (Fluostar Galaxy; BMG Labtechnologies) at 390 nm excitatory and 460 nm emission wavelengths. The background was obtained by incubating tissue samples with 1 µM of the proteasome inhibitor MG132 for 1 h at 37°C. The proteasome activity is expressed as nanomol/minute/milligram protein (mean ± SD).

Statistical analyses

A t test was used for simple comparison. To compare multiple groups to a common control, the one way ANOVA was performed with subsequent posthoc Scheffe's test software, which is available at http://www.analyse-it.com/scheffe-test_y.htm.

References

Beal, M.F., E. Brouillet, B.G. Jenkins, R.J. Ferrante, N.W. Kowall, J.M. Miller, E. Storey, R. Srivastava, B.R. Rosen, and B.T. Hyman. 1993. Neurochemical and histologic characterization of striatal excitotoxic lesions produced by the mitochondrial toxin 3-nitropropionic acid. *J. Neurosci.* 13:4181–4192.

Bence, N.F., R.M. Sampat, and R.R. Kopito. 2001. Impairment of the ubiquitin-proteasome system by protein aggregation. *Science.* 292:1552–1555.

Bulteau, A.L., I. Petropoulos, and B. Friguet. 2000. Age-related alterations of proteasome structure and function in aging epidermis. *Exp. Gerontol.* 35:767–777.

Canu, N., C. Barbato, M.T. Ciotti, A. Serafino, L. Dus, and P. Calissano. 2000. Proteasome involvement and accumulation of ubiquitinated proteins in cerebellar granule neurons undergoing apoptosis. *J. Neurosci.* 20:589–599.

Cooper, J.K., G. Schilling, M.F. Peters, W.J. Herring, A.H. Sharp, Z. Kaminsky, J. Masone, F.A. Khan, M. Delanoy, D.R. Borchelt, et al. 1998. Truncated N-terminal fragments of huntingtin with expanded glutamine repeats form nuclear and cytoplasmic aggregates in cell culture. *Hum. Mol. Genet.* 7:783–790.

Coux, O., K. Tanaka, and A.L. Goldberg. 1996. Structure and functions of the 20S and 26S proteasomes. *Annu. Rev. Biochem.* 65:801–847.

Dardevet, D., C. Sornet, D. Taillandier, I. Savary, D. Attaix, and J. Grizard. 1995. Sensitivity and protein turnover response to glucocorticoids are different in skeletal muscle from adult and old rats. Lack of regulation of the ubiquitin-proteasome proteolytic pathway in aging. *J. Clin. Invest.* 96:2113–2119.

Davies, S.W., M. Turmaine, B.A. Cozens, M. DiFiglia, A.H. Sharp, C.A. Ross, E.

Scherzinger, E.E. Wanker, L. Mangiarini, and G.P. Bates. 1997. Formation of neuronal intranuclear inclusions underlies the neurological dysfunction in mice transgenic for the HD mutation. *Cell.* 90:537–548.

DiFiglia, M., E. Sapp, K.O. Chase, S.W. Davies, G.P. Bates, J.P. Vonsattel, and N. Aronin. 1997. Aggregation of huntingtin in neuronal intranuclear inclusions and dystrophic neurites in brain. *Science.* 277:1990–1993.

Dyer, R.B., and C.T. McMurray. 2001. Mutant protein in Huntington disease is resistant to proteolysis in affected brain. *Nat. Genet.* 29:270–278.

Esler, W.P., and M.S. Wolfe. 2001. A portrait of Alzheimer secretases–new features and familiar faces. *Science.* 293:1449–1454.

Figueiredo-Pereira, M.E., K.A. Berg, and S. Wilk. 1994. A new inhibitor of the chymotrypsin-like activity of the multicatalytic proteinase complex (20S proteasome) induces accumulation of ubiquitin-protein conjugates in a neuronal cell. *J. Neurochem.* 63:1578–1581.

Gafni, J., and L.M. Ellerby. 2002. Calpain activation in Huntington's disease. *J. Neurosci.* 22:4842–4849.

Goffredo, D., D. Rigamonti, M. Tartari, A. De Micheli, C. Verderio, M. Matteoli, C. Zuccato, and E. Cattaneo. 2002. Calcium-dependent cleavage of endogenous wild-type huntingtin in primary cortical neurons. *J. Biol. Chem.* 277: 39594–39598.

Gutekunst, C.A., S.H. Li, H. Yi, J.S. Mulroy, S. Kuemmerle, R. Jones, D. Rye, R.J. Ferrante, S.M. Hersch, and X.J. Li. 1999. Nuclear and neuropil aggregates in Huntington's disease: relationship to neuropathology. *J. Neurosci.* 19:2522–2534.

Hackam, A.S., R. Singaraja, C.L. Wellington, M. Metzler, K. McCutcheon, T. Zhang, M. Kalchman, and M.R. Hayden. 1998. The influence of huntingtin protein size on nuclear localization and cellular toxicity. *J. Cell Biol.* 141: 1097–1105.

Hazeki, N., T. Tsukamoto, I. Yazawa, M. Koyama, S. Hattori, I. Someki, T. Iwatsubo, K. Nakamura, J. Goto, and I. Kanazawa. 2002. Ultrastructure of nuclear aggregates formed by expressing an expanded polyglutamine. *Biochem. Biophys. Res. Commun.* 294:429–440.

Johnston, J.A., C.L. Ward, and R.R. Kopito. 1998. Aggresomes: a cellular response to misfolded proteins. *J. Cell Biol.* 143:1883–1898.

Keller, J.N., F.F. Huang, and W.R. Markesbery. 2000. Decreased levels of proteasome activity and proteasome expression in aging spinal cord. *Neuroscience.* 98:149–156.

Kim, Y.J., Y. Yi, E. Sapp, Y. Wang, B. Cuiffo, K.B. Kegel, Z.H. Qin, N. Aronin, and M. DiFiglia. 2001. Caspase 3-cleaved N-terminal fragments of wild-type and mutant huntingtin are present in normal and Huntington's disease brains, associate with membranes, and undergo calpain-dependent proteolysis. *Proc. Natl. Acad. Sci. USA.* 98:12784–12789.

Lee, D.H., and A.L. Goldberg. 1998. Proteasome inhibitors: valuable new tools for cell biologists. *Trends Cell Biol.* 8:397–403.

Lee, C.K., R. Weindruch, and T.A. Prolla. 2000. Gene-expression profile of the ageing brain in mice. *Nat. Genet.* 25:294–297.

Li, H., S.H. Li, H. Johnston, P.F. Shelbourne, and X.J. Li. 2000. Amino-terminal fragments of mutant huntingtin show selective accumulation in striatal neurons and synaptic toxicity. *Nat. Genet.* 25:385–389.

Li, S.H., A.L. Cheng, H. Li, and X.J. Li. 1999. Cellular defects and altered gene expression in PC12 cells stably expressing mutant huntingtin. *J. Neurosci.* 19: 5159–5172.

Li, S.H., A.L. Cheng, H. Zhou, S. Lam, M. Rao, H. Li, and X.J. Li. 2002. Interaction of Huntington disease protein with transcriptional activator Sp1. *Mol. Cell. Biol.* 22:1277–1287.

Lin, C.H., S. Tallaksen-Greene, W.M. Chien, J.A. Cearley, W.S. Jackson, A.B. Crouse, S. Ren, X.J. Li, R.L. Albin, and P.J. Detloff. 2001. Neurological abnormalities in a knock-in mouse model of Huntington's disease. *Hum. Mol. Genet.* 10:137–144.

Lunkes, A., K.S. Lindenberg, L. Ben-Haiem, C. Weber, D. Devys, G.B. Landwehrmeyer, J.L. Mandel, and Y. Trottier. 2002. Proteases acting on mutant huntingtin generate cleaved products that differentially build up cytoplasmic and nuclear inclusions. *Mol. Cell.* 10:259–269.

Martin-Aparicio, E., A. Yamamoto, F. Hernandez, R. Hen, J. Avila, and J.J. Lucas. 2001. Proteasomal-dependent aggregate reversal and absence of cell death in a conditional mouse model of Huntington's disease. *J. Neurosci.* 21:8772–8781.

Mende-Mueller, L.M., T. Toneff, S.R. Hwang, M.F. Chesselet, and V.Y. Hook. 2001. Tissue-specific proteolysis of Huntingtin (htt) in human brain: evidence of enhanced levels of N- and C-terminal htt fragments in Huntington's disease striatum. *J. Neurosci.* 21:1830–1837.

Orr, H.T. 2001. Beyond the Qs in the polyglutamine diseases. *Genes Dev.* 15:925–932.

Petropoulos, I., M. Conconi, X. Wang, B. Hoenel, F. Bregegere, Y. Milner, and B. Friguet. 2000. Increase of oxidatively modified protein is associated with a decrease of proteasome activity and content in aging epidermal cells. *J. Gerontol. A Biol. Sci. Med. Sci.* 55:B220–B227.

Piccinini, M., O. Tazartes, M. Mostert, A. Musso, M. DeMarchi, and M.T. Rinaudo. 2000. Structural and functional characterization of 20S and 26S proteasomes from bovine brain. *Brain Res. Mol. Brain Res.* 76:103–114.

Sanchez, I., C. Mahlke, and J. Yuan. 2003. Pivotal role of oligomerization in expanded polyglutamine neurodegenerative disorders. *Nature.* 421:373–379.

Schilling, G., M.W. Becher, A.H. Sharp, H.A. Jinnah, K. Duan, J.A. Kotzuk, H.H. Slunt, T. Ratovitski, J.K. Cooper, N.A. Jenkins, et al. 1999. Intranuclear inclusions and neuritic aggregates in transgenic mice expressing a mutant N-terminal fragment of huntingtin. *Hum. Mol. Genet.* 8:397–407.

Starke-Reed, P.E., and C.N. Oliver. 1989. Protein oxidation and proteolysis during aging and oxidative stress. *Arch. Biochem. Biophys.* 275:559–567.

Sun, B., W. Fan, A. Balciunas, J.K. Cooper, G. Bitan, S. Steavenson, P.E. Denis, Y. Young, B. Adler, L. Daugherty, et al. 2002. Polyglutamine repeat length-dependent proteolysis of huntingtin. *Neurobiol. Dis.* 11:111–122.

Vonsattel, J.P., R.H. Myers, T.J. Stevens, R.J. Ferrante, E.D. Bird, and E.P. Richardson, Jr. 1985. Neuropathological classification of Huntington's disease. *J. Neuropathol. Exp. Neurol.* 44:559–577.

Waelter, S., A. Boeddrich, R. Lurz, E. Scherzinger, G. Lueder, H. Lehrach, and E.E. Wanker. 2001. Accumulation of mutant huntingtin fragments in aggresome-like inclusion bodies as a result of insufficient protein degradation. *Mol. Biol. Cell.* 12:1393–1407.

Watase, K., E.J. Weeber, B. Xu, B. Antalffy, L. Yuva-Paylor, K. Hashimoto, M. Kano, R. Atkinson, Y. Sun, D.L. Armstrong, et al. 2002. A long CAG repeat in the mouse Sca1 locus replicates SCA1 features and reveals the impact of protein solubility on selective neurodegeneration. *Neuron.* 34:905–919.

Wellington, C.L., L.M. Ellerby, C.A. Gutekunst, D. Rogers, S. Warby, R.K. Graham, O. Loubser, J. van Raamsdonk, R. Singaraja, Y.Z. Yang, et al. 2002. Caspase cleavage of mutant huntingtin precedes neurodegeneration in Huntington's disease. *J. Neurosci.* 22:7862–7872.

Wessel, D., and U.I. Flugge. 1984. A method for the quantitative recovery of protein in dilute solution in the presence of detergents and lipids. *Anal. Biochem.* 138:141–143.

Wheeler, V.C., J.K. White, C.A. Gutekunst, V. Vrbanac, M. Weaver, X.J. Li, S.H. Li, H. Yi, J.P. Vonsattel, J.F. Gusella, et al. 2000. Long glutamine tracts cause nuclear localization of a novel form of huntingtin in medium spiny striatal neurons in HdhQ92 and HdhQ111 knock-in mice. *Hum. Mol. Genet.* 9:503–513.